Bioorg. Med. Chem. Lett. 38 (2021) 127855

Contents lists available at ScienceDirect

Bioorganic & Medicinal Chemistry Letters

journal homepage: www.elsevier.com/locate/bmcl

Design, synthesis and biological evaluation of mono- and bisquinoline methanamine derivatives as potential antiplasmodial agents

Fostino R.B. Bokosi [a,*], Richard M. Beteck [a,b], Mziyanda Mbaba [a,c], Thanduxolo E. Mtshare [d], Dustin Laming [e], Heinrich C. Hoppe [e,f], Setshaba D. Khanye [a,d,e,*]

[a] Department of Chemistry, Faculty of Science, Rhodes University, Makhanda 6140, South Africa
[b] Centre of Excellence for Pharmaceutical Sciences, North-West University, Potchefstroom 2520, South Africa
[c] Department of Chemistry, Faculty of Science, University of Cape Town, Rondebosch 7701, South Africa
[d] Division of Pharmaceutical Chemistry, Faculty of Pharmacy, Rhodes University, Makhanda 6140, South Africa
[e] Centre for Chemico- and Biomedicinal Research, Rhodes University, Makhanda 6140, South Africa
[f] Department of Biochemistry and Microbiology, Faculty of Science, Rhodes University, Makhanda 6140, South Africa

ARTICLE INFO

Keywords:
Antiplasmodial
Quinoline
Chloroquine-sensitive
Plasmodium falciparum

ABSTRACT

Several classes of antimalarial drugs are currently available, although issues of toxicity and the emergence of drug resistant malaria parasites have reduced their overall therapeutic efficiency. Quinoline based antiplasmodial drugs have unequivocally been long-established and continue to inspire the design of new antimalarial agents. Herein, a series of mono- and bisquinoline methanamine derivatives were synthesised through sequential steps; Vilsmeier-Haack, reductive amination, and nucleophilic substitution, and obtained in low to excellent yields. The resulting compounds were investigated for *in vitro* antiplasmodial activity against the 3D7 chloroquine-sensitive strain of *Plasmodium falciparum*, and compounds **40** and **59** emerged as the most promising with IC_{50} values of 0.23 and 0.93 μM, respectively. The most promising compounds were also evaluated *in silico* by molecular docking protocols for binding affinity to the {001} fast-growing face of a hemozoin crystal model.

Introduction

Malaria is one of the deadliest protozoan diseases transmitted by the female *Anopheles* mosquito. Five species of the genus *Plasmodium* are known to cause malaria infections in humans.[1] These include: *P. falciparum*, *P. vivax*, *P. malariae*, *P. ovale* and *P. knowlesi*. *P. falciparum* is responsible for majority of malaria deaths and is the most prevalent species in sub-Saharan Africa.[2] Despite numerous endeavours to reduce malaria incidence over the last decades, this tropical disease still remains far from being vanquished. According to the 2020 report by World Health Organization (WHO), an estimated 229 million malaria cases and 409 000 malaria deaths were reported worldwide in 2019. Predominantly, the disease has a high toll on pregnant women and children aged under 5 years in sub-Saharan Africa.[1,3–6] Chemotherapeutics have proven to be an effective means of reducing the burden of malaria. Currently, the best available treatments, particularly for uncomplicated and severe malaria infections caused by *P. falciparum* are artemisinin combination therapies (ACTs). In ACTs, a fast-acting, albeit short-lived artemisinin or its semi-synthetic derivatives (dihydroartemisinin, artemether or artesunate) is administered in combination with a longer-lasting partner drug such as amodiaquine, mefloquine, piperaquine, lumefantrine, sulfadoxine and pyrimethamine.[7–9] Although ACTs are highly efficacious with a high pharmacological tolerance profile, several cases of ACTs treatment failure are being reported in parts of South-East Asia.[10] With increasing cases of resistance to available antimalarial agents, intensive drug discovery efforts aimed at developing new antimalarial drugs or modifying existing agents are ongoing. Ideally, highly efficacious, novel antimalarial compounds need to be developed to supplement or replace clinically available drugs.[11–13]

The quinoline scaffold is prominent in most drugs and continues to receive substantial attention in medicinal chemistry due to its broad spectrum of biological activities. Specifically, quinolines have been known to display antimalarial,[14–17] antitubercular,[18] antibacterial,[19] antitrypanosomal,[20] anticancer,[21,22] antifungal[23] and anti-HIV[24] properties. Within the quinoline class, 2,3-disubstituted quinolines have recently gained significant attention as bioactive drug template in malaria drug discovery. Vandekerckhove and colleagues synthesised a

* Corresponding authors at: Department of Chemistry, Faculty of Science, Rhodes University, Makhanda 6140, South Africa (S.D. Khanye).
E-mail addresses: bokosifostino@gmail.com (F.R.B. Bokosi), s.khanye@ru.ac.za (S.D. Khanye).

https://doi.org/10.1016/j.bmcl.2021.127855
Received 14 December 2020; Received in revised form 1 February 2021; Accepted 5 February 2021
Available online 18 February 2021
0960-894X/

novel class of (hydroxyalkylamino)quinoline derivatives *via* cyclisation of diallylaminoquinolines and 4-chloro-*N*-quinolinylbutanamides and investigated their *in vitro* antiplasmodial potential against NF54 chloroquine-sensitive (CQS) strain and Dd2 chloroquine-resistant strain (CQR) of *P. falciparum*.[25] Among the investigated derivatives, 2-methyl-3-(2-methylpyrrolidin-1-yl) quinoline (**1**) was found to be the most potent agent, having IC_{50} values of 13.3 and 38 μM against chemosensitive (NF54) and multidrug-resistant (Dd2) *P. falciparum* strains, respectively. The research team of Patel and Ladani synthesised a library of compounds containing the 2-chloroquinoline nucleus and identified hit compound **2** (0.089 μM) with excellent inhibitory activity against *P. falciparum* comparable to quinine (0.826 μM).[26] Subsequently, Akhter et al (2015) investigated 3-[(2-chloroquinolin-3-yl)methylene]-5-phenylfuran-2(3*H*)-one derivatives (**3**) as antiplasmodial agent targeting *P. falciparum* falcipain-2 (*Pf*FP-2).[27] By conjugating quinoline to a chalcone moiety, Rosenthal and co-workers developed novel class of substituted quinolinyl-chalcone hybrids (**4**) with *in vitro* antimalarial activities.[28] Similarly, Karad et al (2016) prepared 2,3-disubstituted quinoline conjugates under microwave, with derivative **5** possessing impressive antiplasmodial activity against 3D7 *P. falciparum* strain.[29] Arylaminobiquinoline derivatives were synthesised and evaluated for their antimalarial activity against 3D7 strain of *P. falciparum* by Patel and colleagues.[30] Some of them showed antimalarial activity with IC_{50} values as low as 0.005–0.009 μg/mL. The most active compound **6** of the *N*-arylaminobiquinoline derivatives had superior antimalarial activity compared to chloroquine, highlighting the appeal of conjugating two pharmacophoric quinoline units to produce potent plasmocidal compounds (See Fig. 1).

In continuation of our search for new molecules with anti-infective properties,[31–34] we decided to investigate the antiplasmodial properties of novel substituted quinoline derivatives. The quinoline scaffold was derivatized using various simple bioactive, bioisosteric heterocycles, namely: 2-pyridyl, 3-pyridyl, 4-pyridyl, 2-thiophenyl and 2-furfuryl units. Some of these heterocycles have been reported to exhibit excellent antiplasmodial activity.[35–37] The combination of the privileged

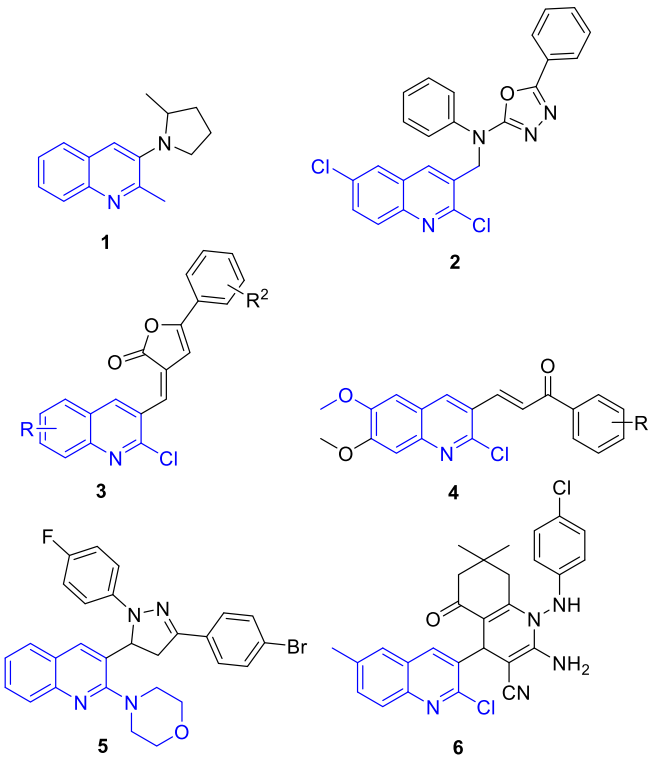

Fig. 1. Representative chemical structures of 2,3-disubstituted quinoline derivatives exhibiting antimalarial activity.

quinoline scaffold (bearing a varied substitution pattern) with a synthetically and biologically suited heterocyclic moiety might reveal new perspectives in development of bioactive compounds. In order to examine the effect of key structural features critical for inhibitory antiplasmodial effects of the compounds and as part of examining structure–activity relationship (SAR), the proposed compounds were designed as highlighted in Fig. 2.

In light of the impressive pharmacological profile of the quinoline scaffold from previous studies, especially for targeting the heme detoxification pathway[38,39] and inhibiting *P. falciparum* falcipain-2 (*Pf*FP2),[40] the quinoline moiety (**A**) served as the core backbone onto which heteroaryl units (**B**) could be appended. Since protonation of quinolinyl antimalarial drugs inside the acidic target site of the parasite digestive vacuole (DV) is important for activity,[15] we incorporated a basic, trimethylamine linker to promote protonation and consequently enhance the antiplasmodial activity of the conceptualised compounds. Positions 2, 5, 6 and 7 of the quinoline scaffold were substituted with various moieties (F, Cl, H, Me, OH and OMe) to probe substitution patterns and electronic effects on the overall activity of the compounds. Lastly, a second quinoline nucleus (**C**) was appended *via* the linker to attain bisquinoline analogues.[41–45] In summary, the design of the target compounds entails: (i) substitution of C-2 of the quinoline scaffold with chloro or methoxy moieties as the core pharmacophoric backbone, (ii) variation of bioisosteric heterocycles appended to C-3 of the quinoline nucleus, (iii) interrogation of electronic and substituents effects on the core quinoline skeleton (mainly at positions −5, −6 and −7) and (iv) generation of bisquinolines. Hence, the objective of this study consists of the design, synthesis and antiplasmodial evaluation of a range of novel substituted mono and bisquinolines. An attempt to explore possible mode of action of this chemical series is also undertaken by assessing the most promising compounds.

Acetanilides **7**–**12** were subjected to Vilsmeier-Haack reaction to afford intermediates **13**–**18** in 36–84% yields.[46] Compounds **13**–**18** were refluxed in a methanolic KOH solution, inducing nucleophilic substitution at the C-2 position to obtain 2-methoxyquinoline-3-carbaldehydes **19**–**24**, which were subsequently subjected to reductive amination with a selection of primary heteroaryl methylamines to form the secondary amines **33**–**51**.[47,48] Treatment of **33**–**51** with corresponding 2-chloromethylquinolines **29**–**32** afforded the desired bisquinolinyl amines **52**–**64** (Scheme 1) in yields ranging 17–82%. Intermediates **29**–**32** were prepared in two consecutive steps: reduction of intermediates **13**–**16** to **25**–**28**, followed by alcohol chlorination. Bisquinolinyl amines **65**–**68** with identical quinoline units were readily obtained *via* double nucleophilic substitution of 2-(aminomethyl)pyridine with 2-chloro-3-(chloromethyl)-6-substituted quinolines **29**–**32** in absolute ethanol in the presence of Et_3N[49] in moderate to excellent yields (Scheme 2). However, substitution of the 2-chloro-3-(chloromethyl)-6-substituted quinolines with the other aminomethyl heterocycles (containing **B** – **E** units shown in Table 1) under similar conditions was unsuccessful. Thus, the 2-methoxy congeners **70**–**72** of these derivatives were achieved by nucleophilic substitution employing the reaction conditions described for synthesis of compounds **19**–**24**. Lastly, demethylation of **67** with BBr_3 under an inert atmosphere yielded the corresponding phenolic analogue **69** in 69% yield.[50]

The structures of all newly synthesised compounds were unambiguously characterised by common spectroscopic techniques: FTIR, ^1H and ^{13}C NMR, 2D NMR and HRMS. The full spectral data of prepared compounds are provided in the Electronic Supporting Information (ESI). The IR spectra of **33**–**51** contain bands *ca* 3370–3240 cm^{-1}, which indicate secondary amine absorption. The broad absorption band around 3206 cm^{-1} in compound **69** is due to the aromatic O—H stretching. The ^1H NMR spectra of *N*-(quinolin-3-ylmethyl)methanamines (**33**–**51**) show a broad singlet *ca* δ 2.86–1.99 ppm, which is diagnostic of the aliphatic N — H group. Disappearance of the aldehydic signals *ca* δ 10.5 ppm (^1H NMR) and δ 189 ppm (^{13}C NMR) observed from the starting materials **19**–**24** and the appearance of two singlet methylene groups *ca* δ

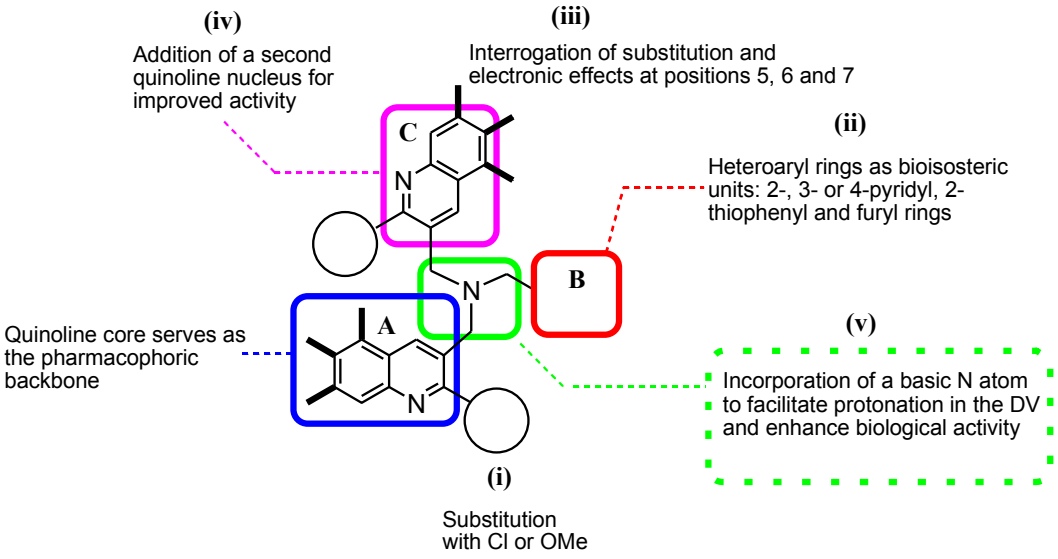

Fig. 2. Design of proposed compounds.

4.09–3.81 ppm, confirmed the transformation of a carbonyl unit into desired amines **33**–**51**. Lastly, a prominent proton signal integrating for two protons for **69** was observed at δ 10.12 ppm assignable to the aromatic OH groups. The molecular ion peaks of all the compounds were observed as protonated molecular ions $[M + H]^+$ corresponding to their respective molecular weights.

All compounds were evaluated for *in vitro* antiplasmodial activity against the CQS (3D7) of *P. falciparum* while cytotoxicity against healthy cells was determined using mammalian HeLa cells. The activities indicated by their corresponding IC_{50} values of the synthesised monoquinoline **33**–**51** and bisquinoline derivatives **52**–**72** along with the activities of the antimalarial drug chloroquine and cytotoxic agent emetine as controls are summarised in Tables 1 and 2, respectively. HeLa cell activity was presented as percentage viability of cells remaining after incubation with 20 μM of the test compounds. In the *N*-(quinolin-3-ylmethyl)methanamine subseries (**33–51**), compounds **33**–**38** featuring 2-furfuryl or 2-thiophenyl bioisosteric heterocyclic systems shed important antiplasmodial insight as were inactive at the maximum tested concentration ($IC_{50} > 20$ μM). With the exception of compounds **41** and **47–48**, all the pyridyl-substituted quinoline derivatives from this subseries exhibited antiplasmodial activity with IC_{50} values in the range of 0.23 – 17.9 μM; with compound **40** exhibiting superior potency with $IC_{50} = 0.23$ μM. Analysis of the data revealed that the 6-membered pyridyl groups promote antiplasmodial activity better than 5-membered counterparts (2-furfuryl and 2-thiophenyl). Antiplasmodial activity seems to increase in the order: 2-pyridyl > 4-pyridyl > 3-pyridy within the pyridyl containing compounds. The influence of substituents at C2, C5, C6 and C7 of the quinoline ring on the antiplasmodial activity was not clear-cut. Most importantly, majority of compounds in the *N*-(quinolin-3-ylmethyl)methanamine subseries (**33–51**) showed little or no cytotoxic effects on the HeLa cell line, exhibiting > 50% cell viability at 20 μM. Although **39** had promising antiplasmodial activity with an IC_{50} value of 1.4 μM against the 3D7 strain, it moderately reduced HeLa cell viability to 44.3% at 20 μM (Table 1).

Next, we generated bisquinoline subseries (**52**–**63**) to investigate the concurrent effect of two quinoline units and a tertiary amine on antiplasmodial activity. As shown in Table 2, the addition of a second quinoline moiety general promotes antiplasmodial activity. This is evident when comparing **33**–**38** (which are all not active, $IC_{50} > 20$ μM) against compounds **58**–**63**, which generally exhibited antiplasmodial activity in the sub-micromolar to low micromolar concentration (with the exception of **61** and **62**, which are inactive; $IC_{50} > 20$ μM). The thiophenyl bisquinoline **59** demonstrated the highest activity ($IC_{50} =$ 0.93 μM) in the entire series despite its mono-quinoline congener (**37**) not showing any discernible activity at the highest tested concentration ($IC_{50} > 20$ μM). Furthermore, we noted that the activity of the previously less active 3-pyridyl variants (**42**, **44**, **45**, **47** and **48**) showed improvement in activity by approximately 2-fold upon coupling of a second quinoline unit (**53–56**). Therefore, it is clear from these observations that the second quinoline unit and a tertiary amine are indeed beneficial for antiplasmodial activity. On the other hand, grafting a second quinoline unit to the 2-pyridyl monoquinolines **39** and **40** did not exert marked effects on the antiplasmodial activity of the resulting compounds (**64** and **70**) albeit displaying somewhat reduced activities. Consequently, these findings further suggest that a trimethylamine linker in lieu of a secondary dimethylamine might be essential for activity. Regarding effects of substituents on the quinoline ring; replacement of 2-Cl with 2-OMe led to increased antiplasmodial activity. For example, replacing the 2-Cl moiety in **65** ($IC_{50} > 20$ μM) and **67** ($IC_{50} >$ 20 μM) with 2-OMe afforded compounds **70**, (IC_{50}: 3.5 μM) and **72** (IC_{50}: 3.4 μM), respectively, with low micromolar antiplasmodial activity. Moreover, substituents at positions C-5, C-6 and C-8 (F, Me, OMe, H, OH and 5,7-diMe) seemed to be tolerated for activity across all compounds, especially the derivatives containing the 2-OMe substituent on the quinoline scaffold, with F and OH being the most favourable substituents (Table 2). Superior antiplasmodial activity of compounds **40** and **59** concurred with several antiprotozoal 2- or 6-methoxy quinolines that have been reported by others in literature.[26,51–58]

To rationalise the possible mechanism of action of the investigated compounds, the most promising compounds **40** and **59** were evaluated *in silico* by molecular docking protocols for binding affinity to the {0 0 1} fast-growing face of a hemozoin crystal model (a validated antimalarial target of quinoline-based drugs) according to previously published methods.[31,59,60] Models of the binding ligands were protonated at pH 4.0 ± 1.0 to mimic the acidic environment inside the DV of the malaria parasite prior to docking. In all cases the nitrogenous linker of the predicted compounds was protonated under the used conditions, which suggests that this moiety may indeed be beneficial for accumulation of the compounds into the parasitic DV and potentially improve their antimalarial activity by pH trapping.[15] Examples of generated diprotonated states of the compounds at both the quinoline and linker N atoms are shown in Fig. 3**A, B**. Both compounds exhibited high affinity for the {0 0 1} hemozoin side face, forming multiple π-assisted contacts (π-π, π-anion/cation, π-alkyl) with the heme moieties inside the crevices of this corrugated face (Fig. 3**C, D**). This is further substantiated by the negative docking scores of –9.23 and –8.41 kcal/mol for **40** and **59**,

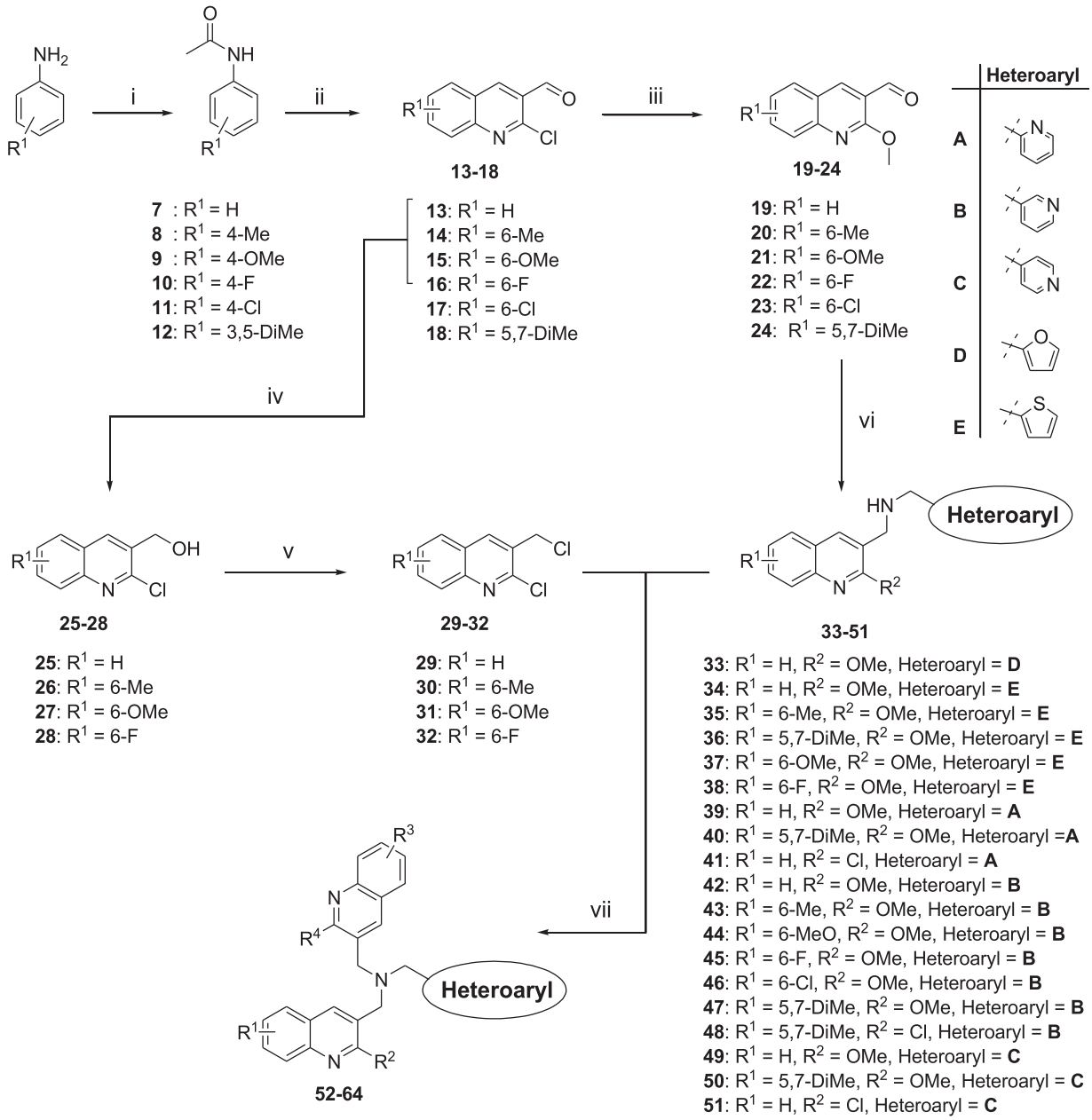

7 : R^1 = H
8 : R^1 = 4-Me
9 : R^1 = 4-OMe
10: R^1 = 4-F
11: R^1 = 4-Cl
12: R^1 = 3,5-DiMe

13: R^1 = H
14: R^1 = 6-Me
15: R^1 = 6-OMe
16: R^1 = 6-F
17: R^1 = 6-Cl
18: R^1 = 5,7-DiMe

19: R^1 = H
20: R^1 = 6-Me
21: R^1 = 6-OMe
22: R^1 = 6-F
23: R^1 = 6-Cl
24: R^1 = 5,7-DiMe

25: R^1 = H
26: R^1 = 6-Me
27: R^1 = 6-OMe
28: R^1 = 6-F

29: R^1 = H
30: R^1 = 6-Me
31: R^1 = 6-OMe
32: R^1 = 6-F

33: R^1 = H, R^2 = OMe, Heteroaryl = **D**
34: R^1 = H, R^2 = OMe, Heteroaryl = **E**
35: R^1 = 6-Me, R^2 = OMe, Heteroaryl = **E**
36: R^1 = 5,7-DiMe, R^2 = OMe, Heteroaryl = **E**
37: R^1 = 6-OMe, R^2 = OMe, Heteroaryl = **E**
38: R^1 = 6-F, R^2 = OMe, Heteroaryl = **E**
39: R^1 = H, R^2 = OMe, Heteroaryl = **A**
40: R^1 = 5,7-DiMe, R^2 = OMe, Heteroaryl =**A**
41: R^1 = H, R^2 = Cl, Heteroaryl = **A**
42: R^1 = H, R^2 = OMe, Heteroaryl = **B**
43: R^1 = 6-Me, R^2 = OMe, Heteroaryl = **B**
44: R^1 = 6-MeO, R^2 = OMe, Heteroaryl = **B**
45: R^1 = 6-F, R^2 = OMe, Heteroaryl = **B**
46: R^1 = 6-Cl, R^2 = OMe, Heteroaryl = **B**
47: R^1 = 5,7-DiMe, R^2 = OMe, Heteroaryl = **B**
48: R^1 = 5,7-DiMe, R^2 = Cl, Heteroaryl = **B**
49: R^1 = H, R^2 = OMe, Heteroaryl = **C**
50: R^1 = 5,7-DiMe, R^2 = OMe, Heteroaryl = **C**
51: R^1 = H, R^2 = Cl, Heteroaryl = **C**

52: R^1 = H, R^2 = OMe, R^3 = H, R^4 = Cl, Heteroaryl = **A**
53: R^1 = H, R^2 = OMe, R^3 = 6-Me, R^4 = Cl, Heteroaryl = **B**
54: R^1 = 6-F, R^2 = OMe, R^3 = 6-Me, R^4 = Cl, Heteroaryl = **B**
55: R^1 = 5,7-DiMe, R^2 = OMe, R^3 = 6-Me, R^4 = Cl, Heteroaryl = **B**
56: R^1 = 5,7-DiMe, R^2 = Cl, R^3 = 6-Me, R^4 = Cl, Heteroaryl = **B**
57: R^1 = 6-Me, R^2 = OMe, R^3 = 6-Me, R^4 = Cl, Heteroaryl = **E**
58: R^1 = 6-Me, R^2 = OMe, R^3 = 6-MeO, R^4 = Cl, Heteroaryl = **E**
59: R^1 = 6-MeO, R^2 = OMe, R^3 = 6-Me, R^4 = Cl, Heteroaryl = **E**
60: R^1 = 6-F, R^2 = OMe, R^3 = 6-Me, R^4 = Cl, Heteroaryl = **E**
61: R^1 = 5,7-DiMe, R^2 = OMe, R^3 = 6-Me, R^4 = Cl, Heteroaryl = **E**
62: R^1 = 5,7-DiMe, R^2 = OMe, R^3 = 6-MeO, R^4 = Cl, Heteroaryl = **E**
63: R^1 = H, R^2 = OMe, R^3 = Me, R^4 = Cl, Heteroaryl = **D**
64: R^1 = 5,7-DiMe, R^2 = OMe, R^3 = 5,7-DiMe, R^4 = OMe, Heteroaryl = **A**

Scheme 1. Reagents and conditions: (i) Ac_2O, AcOH, reflux, 30 min; (ii) DMF/$POCl_3$, 80 °C, 5–18 h; (iii) MeOH/KOH, 60 °C, 2.5–6 h; (iv) MeOH, $NaBH_4$, r.t., 30 min; (v) $SOCl_2$, DCM, 50 °C, 6 h; (vi) heteroaryl methylamine, EtOH, AcOH (cat), 78 °C, 12–48 h followed by EtOH, $NaBH_4$, r.t. 6 h; (vii) EtOH, TEA, 78 °C, 12–18 h.

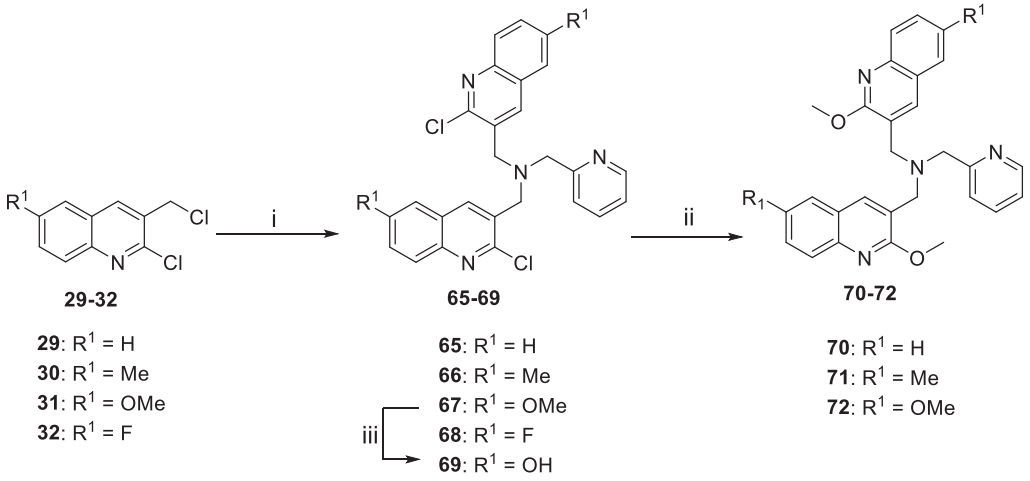

Scheme 2. Synthesis of bisquinolines with identical quinoline nuclei. Reagents and conditions: (i) 2-(Aminomethyl)pyridine, EtOH, Et_3N, 78 °C, 36–48 h; (ii) MeOH/NaH, 70 °C, 36 h; (iii) BBr_3 in DCM (1.0 M), −78 °C, N_2, 30 min → r.t., 3 h.

Table 1
Structures of compounds **33–51**, IC_{50} values against 3D7 strain of *P. falciparum* and % viability of HeLa cells at 20 μM.

Compd	Structure	3D7 IC_{50} (μM)[a]	% HeLa Viability[a]	Compd	Structure	3D7 IC_{50} (μM)[a]	% HeLa Viability[a]
33	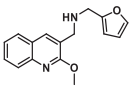	>20	88.9 ± 3.33	**43**	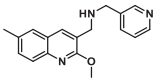	13.4 ± 1.47	99.5 ± 5.98
34	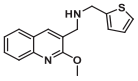	>20	89.9 ± 5.15	**44**	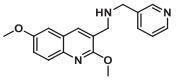	12.8 ± 1.28	100.4 ± 7.18
35	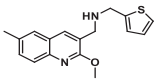	>20	99.7 ± 2.19	**45**	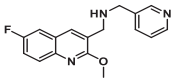	17.9 ± 1.98	97.2 ± 5.59
36	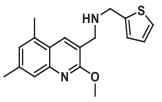	>20	87.5 ± 5.93	**46**	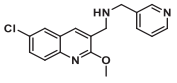	16.8 ± 1.61	100.5 ± 4.89
37	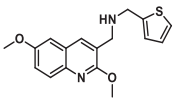	>20	93.2 ± 12.79	**47**	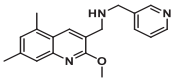	>20	76.7 ± 7.64
38	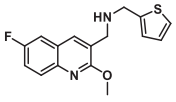	>20	93.5 ± 2.60	**48**	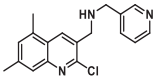	>20	77.23 ± 3.62
39	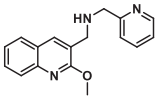	**1.40 ± 0.07**	**44.3 ± 1.31**	**49**	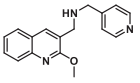	**2.10 ± 0.56**	**69.9 ± 5.93**
40	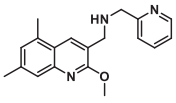	**0.23 ± 0.02**	**56.7 ± 3.25**	**50**	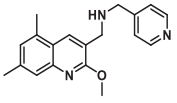	12.0 ± 1.16	60.7 ± 2.31
41	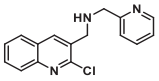	>20	65.6 ± 1.65	**51**	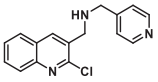	**2.30 ± 0.61**	**73.7 ± 6.25**
42	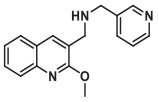	13.4 ± 0.31	89.9 ± 1.22	**Chloroquine**	–	0.023	–
				Emetine	–	–	0.013

respectively, which illustrates a trend correlating with the observed antiplasmodial activity evaluated on the 3D7 *P. falciparum* strain, i.e., **40** (0.23 μM) > **59** (0.93 μM).

Herein, we reported the synthesis of thirty nine structurally simple quinoline derivatives and evaluated them for their *in vitro* antiplasmodial activity against the 3D7 strain of *P. falciparum*. Bioassay screening culminated in the identification of hit compounds **40** and **59**, which displayed IC_{50} values in the sub-micromolar range. The SAR

Table 2
Structures of compounds **52–72**, IC_{50} values against 3D7 strain of *P. falciparum* and % viability of HeLa cells at 20 μM.

Compd.	Structure	3D7 IC_{50} (μM)[a]	% HeLa Viability[a]	Compd	Structure	3D7 IC_{50} (μM)[a]	% HeLa Viability[a]
52	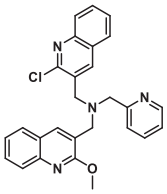	>20	89.9 ± 11.98	**64**	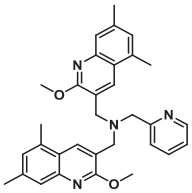	2.80 ± 0.18	90.1 ± 4.71
53	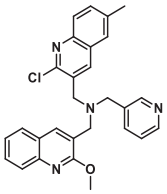	9.80 ± 1.24	98.3 ± 8.65	**65**	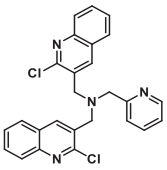	>20	90.6 ± 12.56
54	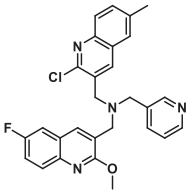	9.60 ± 1.12	92.6 ± 10.76	**66**	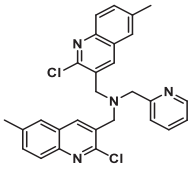	>20	93.0 ± 2.02
55	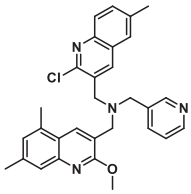	12.3 ± 1.32	77.6 ± 11.9	**67**	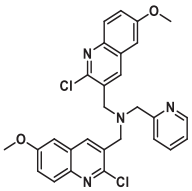	>20	83.8 ± 9.01
56	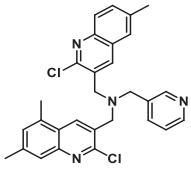	7.60 ± 0.73	80.3 ± 4.66	**68**	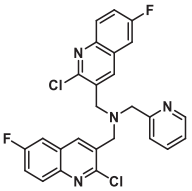	9.80 ± 1.23	98.7 ± 9.56
57	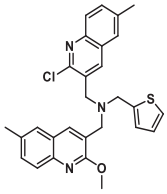	12.6 ± 1.51	87.9 ± 3.35	**69**	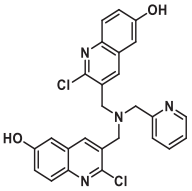	**2.50 ± 0.41**	88.8 ± 9.74
58	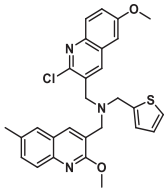	13.4 ± 1.74	103.2 ± 3.95	**70**	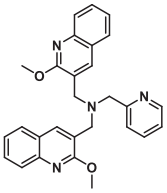	3.50 ± 0.12	89.0 ± 8.79
59	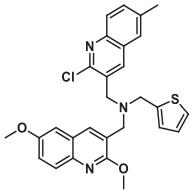	**0.93 ± 0.04**	99.2 ± 4.74	**71**	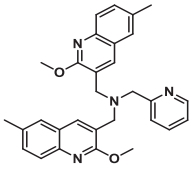	>20	93.3 ± 11.5
60	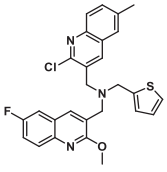	11.3 ± 1.18	95.2 ± 1.08	**72**	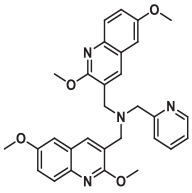	3.40 ± 0.71	79.5 ± 0.93

(*continued on next page*)

Table 2 (*continued*)

Compd.	Structure	3D7 IC_{50} (μM)[a]	% HeLa Viability[a]	Compd	Structure	3D7 IC_{50} (μM)[a]	% HeLa Viability[a]
61	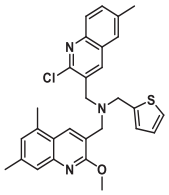	>20	86.0 ± 7.17	**Chloroquine**	–	0.023	–
62	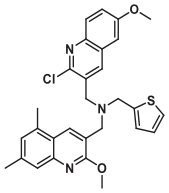	>20	85.4 ± 2.97	**Emetine**	–	–	0.013
63	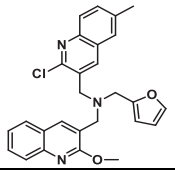	12.8 ± 1.11	84.4 ± 3.37				

[a] The values are the mean ± SD of experiments performed in triplicate.

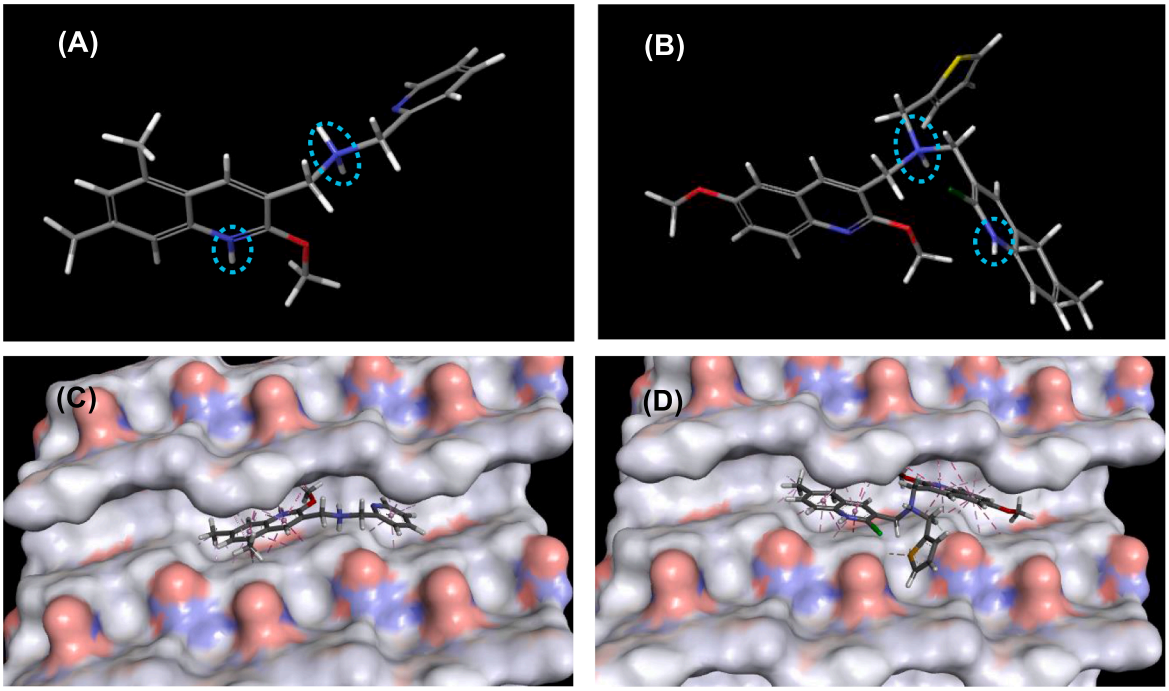

Fig. 3. Results of the computational simulation study. (**A-B**) Examples of predicted forms of the compounds diprotonated at N atoms of the quinoline and linker motifs. (**C-D**) Low-energy binding conformations of protonated structures (at pH 4.0 ± 1.0) of compounds **40** and **59** bound to the {0 0 1} fast-growing face of the hemozoin crystal interacting with the heme moieties.

analysis suggest that the introduction of a second quinoline moiety significantly promoted both antiplasmodial activity and low cytotoxicity towards the HeLa cell line at 20 μM. Computational molecular docking simulation of tool compounds **40** and **59** suggests hemozoin binding as a plausible mechanism of action of the investigated compounds. The enriched SAR profile obtained from this study, as well as the convenient preparation of these compounds, make the reported organic frameworks attractive in antimalarial drug discovery and warrant further exploration and mechanistic evaluation to fully comprehend their plasmocidal effects.

Declaration of Competing Interest

The authors declare that they have no known competing financial interests or personal relationships that could have appeared to influence the work reported in this paper.

Acknowledgements

Financial support for the chemistry component of this project was provided by the Rhodes University Sandisa Imbewu fund (SDK, HCH),

the National Research Foundation of South Africa and Thuthuka National Research Foundation (Grant No. 107270, SDK). The South African Medical Research Council (SAMRC) funded the antiplasmodial and HeLa cytotoxicity bioassay component of the project. FRBB gratefully acknowledges financial support from the Malawi Government Scholarship Fund and Chancellor College, one of the constituent colleges of the University of Malawi. Authors thank Dr. Tendamudzimu Tshiwawa (Postdoc, Rhodes University) for assistance with computational molecular docking.

Appendix A. Supplementary data

Supplementary data to this article can be found online at https://doi.org/10.1016/j.bmcl.2021.127855.

References

1 Singh B, Daneshvar C. *Clin Microbiol Rev*. 2013;26:165–184.
2 White NJ. *Clin Infect Dis*. 2008;46:172–173.
3 World Health Organization, World malaria report, Geneva, 2019.
4 Qin H-L, Zhang Z-W, Lekkala R, Alsulami H, Rakesh KP. *Eur J Med Chem*. 2020;193, 112215.
5 Cox FEG. *Parasites Vectors*. 2010;3:5.
6 Visser BJ, van Vugt M, Grobusch MP. *Expert Opin Pharmacother*. 2014;15:2219–2254.
7 Eastman RT, Fidock DA. *Nat Rev Microbiol*. 2009;7:864–874.
8 Nosten F, White NJ. *Am J Trop Med Hyg*. 2007;77:181–192.
9 World Health Organization, Guidelines for the treatment of malaria, Geneva, 2015.
10 World Health Organization, Artemisinin resistance and artemisinin-based combination therapy efficacy: status report, 2018.
11 Menard D, Dondorp A. *Cold Spring Harb Perspect Med*. 2017;7, a025619.
12 Ross LS, Fidock DA. *Cell Host Microbe*. 2019;26:35–47.
13 Phillips MA, Rathod PK. *Infect Disord Drug Targets*. 2010;10:226–239.
14 Foley M, Tilley L. *Pharmacol Ther*. 1998;79:55–87.
15 Egan TJ. *Expert Opin Ther Pat*. 2001;11:185–209.
16 Kaur K, Jain M, Reddy RP, Jain R. *Eur J Med Chem*. 2010;45:3245–3264.
17 Baragaña B, Hallyburton I, Lee MCS, et al. *Nature*. 2015;522:315–320.
18 Keri RS, Patil SA. *Biomed Pharmacother*. 2014;68:1161–1175.
19 Marella A, Tanwar OP, Saha R, et al. *Saudi Pharm J*. 2013;21:1–12.
20 Chanquia SN, Larregui F, Puente V, Labriola C, Lombardo E, García Liñares G. *Bioorg Chem*. 2019;83:526–534.
21 Afzal O, Kumar S, Haider MR, et al. *Eur J Med Chem*. 2015;97:871–910.
22 Kaalin G, Suhas AS, Neil AK. *Anti-Cancer Agents Med Chem*. 2015;15:631–646.
23 Musiol R, Serda M, Hensel-Bielowka S, Polanski J. *Curr Med Chem*. 2010;17:1960–1973.
24 Nisha C, Sourav K, Monika C, Raj K. *Mini-Rev Med Chem*. 2019;19:510–526.
25 Vandekerckhove S, Van Herreweghe S, Willems J, et al. *Eur J Med Chem*. 2015;92:91–102.
26 Ladani GG, Patel MP. *New J Chem*. 2015;39:9848–9857.
27 Akhter M, Saha R, Tanwar O, Mumtaz Alam M, Zaman MS. *Med Chem Res*. 2015;24:879–890.
28 Dominguez JN, Charris JE, Lobo G, et al. *Eur J Med Chem*. 2001;36:555–560.
29 Karad SC, Purohit VB, Thakor P, Thakkar VR, Raval DK. *Eur J Med Chem*. 2016;112:270–279.
30 Shah NM, Patel MP, Patel RG. *Eur J Med Chem*. 2012;54:239–247.
31 Mbaba M, Dingle LMK, Swart T, et al. *ChemBioChem*. 2020;21:2643–2658. https://doi.org/10.1002/cbic.202000132.
32 Mbaba M, Dingle LMK, Cash D, et al. *Eur J Med Chem*. 2020;187:111924.
33 Darrell OT, Hulushe ST, Mtshare TE, et al. *S Afr J Chem*. 2018;71:174–181.
34 Zulu AI, Oderinlo OO, Kruger C, et al. *Molecules*. 2020;25:1668.
35 Rice DR, Mendiola MDLB, Murillo-Solano C, Checkley LA, Ferdig MT, Pizarro JC, Smith BD. *Bioorg Med Chem*. 2017;25:2754–2760.
36 Glans L, Ehnbom A, De Kock C, et al. *Dalton Trans*. 2012;41:2764–2773.
37 Gilson PR, Tan C, Jarman KE, et al. *J Med Chem*. 2017;60:1171–1188.
38 Sullivan DJ. *PNAS*. 2017;114:7483–7485.
39 Herraiz T, Guillén H, González-Peña D, Arán VJ. *Sci Rep*. 2019;9:1–16.
40 Singh A, Kalamuddin M, Mohmmed A, Malhotra P, Hoda N. *RSC Adv*. 2019;9:39410–39421.
41 Liebman KM, Burgess SJ, Gunsaru B, et al. *Molecules*. 2020;25:2251.
42 Kondaparla S, Agarwal P, Srivastava K, Puri SK, Katti SB. *Chem Bio Drug Des*. 2017;89:901–906.
43 Fielding AJ, Evans P, Alizadeh S, et al. *Chem Eur J*. 2017;23:6811–6828.
44 Van Heerden L, Cloete TT, Breytenbach JW, et al. *Eur J Med Chem*. 2012;55:335–345.
45 Kaur K, Jain M, Khan SI, et al. *Bioorg Med Chem*. 2011;19:197–210.
46 Meth-Cohn O, Narine B, Tarnowski B. J Chem Soc. *Perkin Trans*. 1981;1:1520–1530.
47 Kuethe JT, Wong A, Qu C, Smitrovich J, Davies IW, Hughes DL. *J Org Chem*. 2005;70:2555–2567.
48 Jain PP, Degani MS, Raju A, Ray M, Rajan M. *Bioorg Med Chem Lett*. 2013;23:6097–6105.
49 Kumar S, Bawa S, Drabu S, Gupta H, Machwal L, Kumar R. *Eur J Med Chem*. 2011;46:670–675.
50 Choi W-K, El-Gamal MI, Choi HS, Baek D, Oh C-H. *Eur J Med Chem*. 2011;46:5754–5762.
51 Upadhayaya RS, Vandavasi JK, Vasireddy NR, Sharma V, Dixit SS, Chattopadhyaya J. *Bioorg Med Chem*. 2009;17:2830–2841.
52 Mitton-Fry MJ, Brickner SJ, Hamel JC, et al. *Bioorg Med Chem Lett*. 2017;27:3353–3358.
53 Carroll FI, Berrang B, Linn CP, Twine Jr CE. *J Med Chem*. 1979;22:694–699.
54 Carroll FI, Berrang BD, Linn CP. *J Med Chem*. 1980;23:581–584.
55 Drake NL, Van Hook J. *J Am Chem Soc*. 1946;68:1529–1531.
56 Bawa S, Kumar S, Drabu S, Kumar R. *J Pharm Bioallied Sci*. 2010;2:64–71.
57 Panda SS, Bajaj K, Meyers MJ, Sverdrup FM, Katritzky AR. *Org Biomol Chem*. 2012;10:8985–8993.
58 Upadhayaya RS, Dixit SS, Földesi A, Chattopadhyaya J. *Bioorg Med Chem Lett*. 2013;23:2750–2758.
59 Veale CG, Jayram J, Naidoo S, et al. *RSC Med Chem*. 2020;11:85–91.
60 L'abbate FP, Müller R, Openshaw R, et al. *Eur J Med Chem*. 2018;159:243–254.